

Inhibition of Ligand Binding Ability of Three Porphyrins by an Organic Effector

Tomoaki Nishimura, Yoshito Sasaki, Yoshimitsu Tachi, Shuichi Suzuki, Keiji Okada, Masatoshi Kozaki

Citation	Chemistry - An Asian Journal. 15(5); 594-600
Issue Date	2020-03-02
Version of Record	2020-01-28
Type	Journal Article
Textversion	Author
Supporting Information	Supporting information is available at https://doi.org/10.1002/asia.201901711 .
Rights	This is the peer reviewed version of the following article: Chemistry - An Asian Journal Vol.15, Issu.5, p.594-600, which has been published in final form at https://doi.org/10.1002/asia.201901711 . This article may be used for non-commercial purposes in accordance with Wiley Terms and Conditions for Use of Self-Archived Versions.
DOI	10.1002/asia.201901711

Self-Archiving by Author(s)
Placed on: Osaka City University

Inhibition of Ligand Binding Ability of Three Porphyrins by an Organic Effector

Tomoaki Nishimura,^[a] Yoshito Sasaki,^[a] Yoshimitsu Tachi,^[a] Shuichi Suzuki,^[c] Keiji Okada,^{[a], [b]} Masatoshi Kozaki^{*, [a], [b]}

[a] T. Nishimura, Y. Sasaki, Dr. Y. Tachi, Prof. Dr. K. Okada, Prof. Dr. M. Kozaki
Graduate School of Science,
Osaka City University
Sugimoto, Sumiyoshi-ku, Osaka 558-8585 (Japan)
E-mail: kozaki@sci.osaka-cu.ac.jp

[b] Prof. Dr. K. Okada, Prof. Dr. M. Kozaki
Osaka City University Advanced Research Institute for Natural Science and Technology (OCARINA)
Sugimoto, Sumiyoshi-ku, Osaka 558-8585 (Japan)

[c] Dr. S. Suzuki
Graduate School of Engineering Science
Osaka University
Toyonaka, Osaka 560-8531 (Japan)

Supporting information for this article is given via a link at the end of the document.

Abstract: A stimulus-responsive receptor **1** was designed and prepared to control the ligand-binding ability of three active sites, two zinc tetraphenylporphyrin units (P1) and one zinc diethynylphenylporphyrin unit (P2), with one effector molecule **2**. Bulky hexarylbenzene units are incorporated as shielding panels in the middle of the flexible side arms of **1**. Spectroscopic titrations indicated that a stable supramolecular complex **1**·**2** ($K_{1:2} = 6.7 \times 10^6 \text{ M}^{-1}$) was produced via the cooperative formation of multiple hydrogen and coordination bonds. As the result, the binding of a ligand to P1 was inhibited by **2** in a competitive manner. Additionally, the formation of **1**·**2** brought about conformational restriction of the side arms to cover both faces of P2 with the shielding panels. The binding constant of 4-phenylpyridine with P2 in **1**·**2** decreased to 8.9% of that in **1**. Namely, the ligand-binding ability of P2 was inhibited according to an allosteric mechanism.

Introduction

Some enzymes transform their structures by recognizing chemical stimuli at sites other than the binding sites of ligands, which leads to a change in their ligand-binding activity (allosteric regulation).^[1] The allosteric regulation mechanism is a rich source of inspiration for the design of stimulus-responsive receptors and catalysts.^[2,3] Metal cations have been popular chemical stimuli in artificial systems because metal complexations generate strong driving force to bring about conformational transformation.^[3] In nature, molecular recognition is a common trigger for regulating the activity of active sites in allosteric enzymes. There are, however, a limited number of reports of artificial allosteric systems where molecular recognition brought about the conformational transformation.^[4] One reason for this is that it is usually difficult to generate enough driving force to transform the conformation through molecular recognition because it is achieved with weak chemical bond and/or bonding interaction.

In popular artificial allosteric receptors, association of an external chemical stimulus leads to the construction or destruction of preorganized ligand-binding sites to express a

positive or negative effect on their activity, respectively.^[4] On the other hand, Mirkin et al. applied their weak-link concepts to the development of an allosteric catalyst where accessibility of a substrate to an active site was altered with shielding units.^[5] While the shielding strategy is versatile and reliable to switch the activity, a few artificial allosteric systems can be operated by the shielding mechanism.

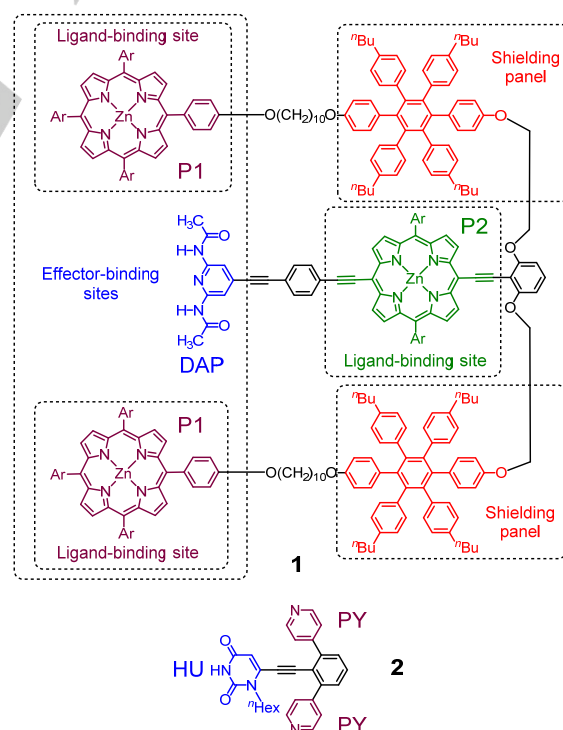


Figure 1. Chemical structures of receptor **1** and effector **2** (Ar = 3,5-di-*tert*-butylphenyl).

Recently, we reported stimulus-responsive receptor that has a zinc 5,15-diethynyl-10,20-diphenylporphyrin unit (P0) as ligand

binding sites (Scheme S1).^[6] Activity of this sites was suppressed by neutral organic molecule (effector). The binding constant of 4-phenylpyridine with P0, however, reduced only by 0.24 times by the effector. Here, we designed closely related receptor **1** with a pair of sterically bulky shielding panels to enhance the degree of the allosteric inhibition by organic effector **2** (Figure 1). Although the side chains of **1** appear to be conformationally flexible, steric bulkiness of the shielding units is probably a dominant factor in the allosteric inhibition.^[7] Absorption spectral titrations were performed to see the stability of the 1:1 supramolecular complex **1•2** and to evaluate the ability of the ligand-binding sites in both **1** and **1•2**. We successfully obtained considerable enhancement in the degree of allosteric inhibition.

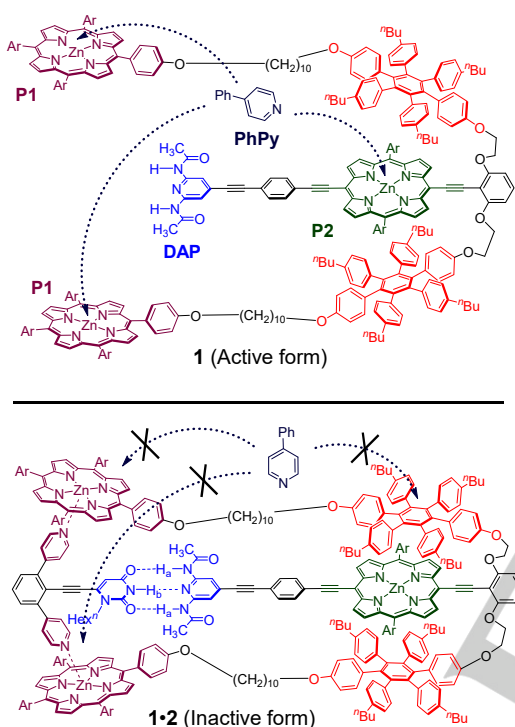


Figure 2. Active and inactive forms of receptor **1**.

Results and Discussion

Receptor **1** is composed of a linear rigid main rod that has a pair of flexible side arms at one end and a diamidopyridine unit (DAP) at the other end (Figure 1). A sterically bulky shielding panel is incorporated in the middle of each side arm. There are two types of ligand-binding sites in **1**: zinc 5,10,15,20-tetraphenylporphyrin units (P1) at the terminal of each side arm and a zinc 5,15-diethynyl-10,20-diphenylporphyrin unit (P2) at the middle of the main rod. Effector **2** possesses two types of binding units that are a couple of 4-pyridyl (PY) groups and one 1-hexyl-uracil group (HU). It is expected that the ligand-binding ability of **1** is inhibited by **2** according to the following mechanism (Figure 2). The association of **1** with **2** produces a stable supramolecular complex **1•2** where both the P1s have coordination bonds with PYs, and DAP forms multiple hydrogen bonds with HU. The binding of ligands to P1 is inhibited in a competitive manner thanks to the high stability of **1•2**. In addition, the formation of **1•2** is accompanied by a large conformational

transformation in the side arms, which results in both the faces of P2 being covered with the shielding panels. As a result, the ligand-binding ability of P2 is allosterically inhibited.

First, we performed semi-empirical calculations using the PM6 method to check for suitable alkyl chain lengths for the formation of the stable supramolecular complex (Table S2). The results suggested that receptor **1** with decamethylene chains $-(CH_2)_{10}-$ between P1, and the shielding panel is the most suitable for producing the stable supramolecular complex with **2**. The energy-minimized structure of **1•2** in Figure 3 suggests that the shielding panels reduce accessibility of ligands to P2. These results indicated that **2** can be a good effector for suppressing the ligand-binding ability of **1**.

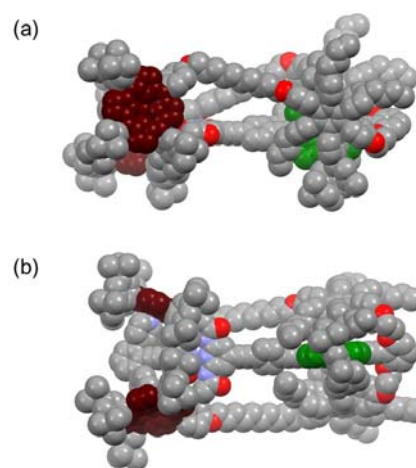
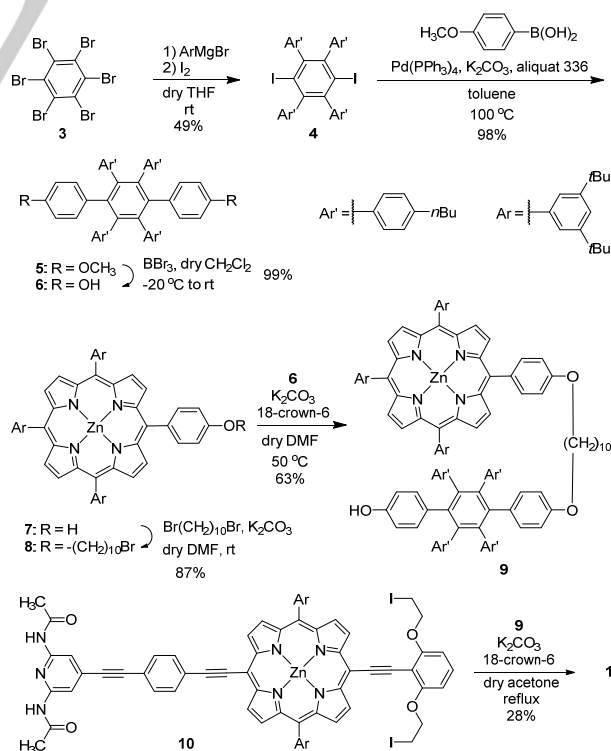


Figure 3. (a) Side and (b) top views of optimized structure of **1•2** (PM6). Carbon, oxygen, and nitrogen atoms are gray, red, blue, and yellow, respectively. P1 and P2 units are purple and green, respectively. All hydrogen atoms are omitted for clarity.



Scheme 1. Synthesis of receptor **1**.

The synthesis of **1** is summarized in Scheme 1. Hexaarylbenzene **6** was obtained from hexabromobenzene (**3**) using the method reported for the synthesis of hexaarylbenzene derivatives.^[8] The reaction of porphyrin **7**^[9] with excess 1,10-dibromodecane under basic conditions afforded porphyrin **8**. Substitution of the bromo group in porphyrin **8** with one of the two hydroxyl groups in hexaarylbenzene **6** was carried out using the Williamson ether synthesis conditions. Side arm **9** and main rod **10** were heated in acetone in the presence of potassium carbonate and 18-crown-6 to produce **1** in 28% yield. The structure of **1** was unambiguously characterized by NMR (Figures S6-S11) and MALDI-TOF MS analyses (Figure S28).

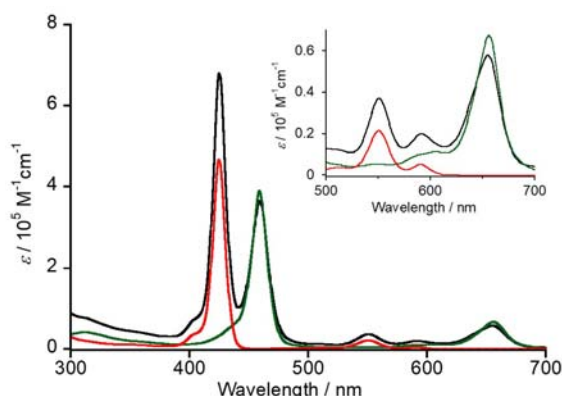


Figure 4. UV-vis spectra of **1**, **9**, and **10** in toluene at 25 °C.

UV-vis spectra of **1**, **9**, and **10** in toluene at 25 °C are displayed and compared in Figure 4. A solution of **1** showed a couple of intense absorption bands at 425 (log ϵ = 5.83) and 459 nm (log ϵ = 5.56) that are attributed to the Soret bands of P1 and P2, respectively.^[10] Three absorption bands with relatively weak intensity were observed at λ_{max} = 551 (log ϵ = 4.64), 592 (log ϵ = 4.34), and 655 nm (log ϵ = 4.88). These bands were reasonably assigned to the Q-band of P1, overlapped absorption of the Q-bands of P1 and P2, and the Q-band of P2, respectively.^[10] These characteristic bands are useful to monitor the ligand binding to P1 and P2 at the same time (vide infra).

First, we investigated the stability of **1**·**2** in toluene (Figure S3). Figure 5(a) shows the absorption spectral change of the solution of **1** (9.98×10^{-6} M) observed after adding up to 1.0 equivalent of **2** (6.05×10^{-4} M). The peak intensities at 551 and 655 nm decreased, and a couple of absorption bands appeared at 563 and 604 nm. During the addition, an isobestic point was observed at 558 nm. It has been established that axial coordination of ligands with zinc porphyrins produces absorption bands in longer wavelength region compared to the corresponding bands of ligand-free zinc porphyrins.^[11] The observed absorption change indicates the axial coordination of PY on the zinc atom of P1. On the other hand, blue shift and a decrease in intensity were observed at λ_{max} = 655 nm which is assigned to P2, indicating the interaction between the shielding panel and P2.^[6] The coordination between PY and P2 is insignificant under these conditions because of the negligible intensity of a characteristic band in the wavelength region longer than 655 nm by the axial coordination.^[11] The binding constant of **1**·**2** was evaluated as $K_{1,2} = 6.73 \pm 0.67 \times 10^6 \text{ M}^{-1}$ from the global curve-fitting by the theoretical curves obtained from the 1:1 binding model ($\mathbf{1} + \mathbf{2} \rightleftharpoons \mathbf{1} \cdot \mathbf{2}$).^[12] These results indicate the

nearly quantitative formation of **1**·**2** under these conditions. The large binding constant between **1** and **2** indicates that the HU-DAP hydrogen bonds and the PY-P1 coordination bonds were cooperatively formed under these conditions.

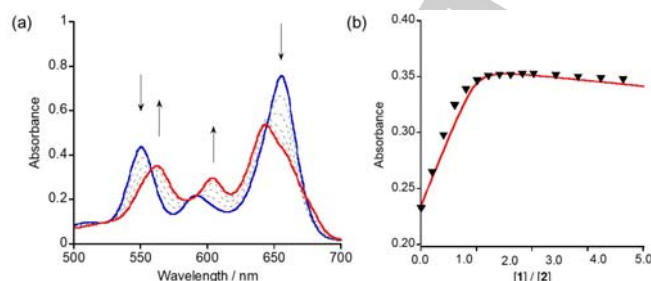


Figure 5. (a) UV-vis spectral titration data of **1** (9.98×10^{-6} M) with **2** (6.05×10^{-4} M) in toluene at 25 °C (0 equiv: blue line, 1.0 equiv: red line) (b) The change in the absorbance at 563 (black inverted triangle) as a function of relative concentration of **2**. The red solid lines are theoretical binding curves obtained by the curve fittings.

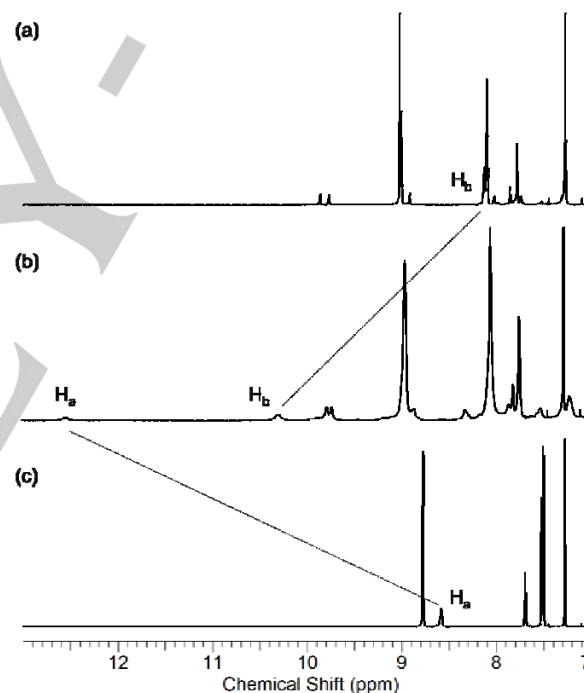


Figure 6. Partial ^1H NMR spectra of (a) **1**, (b) **1**·**2** and (c) **2** in CDCl_3 .

To obtain further insight into the binding of **1** and **2**, ^1H NMR of **1**·**2** was measured in CDCl_3 (Figures S12-S15). NMR spectra of **1**, **2**, and **1**·**2** are displayed and compared in Figure 6. The N–H protons H_a (10.3 ppm) and H_b (12.5 ppm) in **1**·**2** resonated in the lower magnetic field as compared to the N–H proton in **1** (8.12 ppm) and **2** (8.63 ppm), respectively, indicating the formation of multiple hydrogen bonds between DAP and HU.^[13] The NOESY spectrum of **1**·**2** (Figure S1) revealed a clear cross-peak between these signals, indicating that protons H_a and H_b are close to each other. In addition, the NOESY spectrum of **1**·**2** (Figure S2) showed cross-peaks between the signals of aromatic protons in the shielding panel and the signals of β -protons of P2, suggesting that they were in close proximity.

These results are consistent with the quantitative formation of **1**•**2**, where the shielding panels cover both faces of P2.

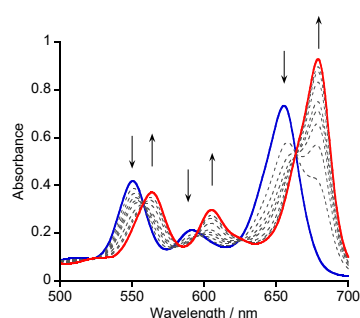


Figure 7. UV-vis spectral change resulting from the titration of **1** (9.81×10^{-6} M) with 4-phenylpyridine in toluene at 25 °C (0 equiv: blue line, 100 equiv: red line).

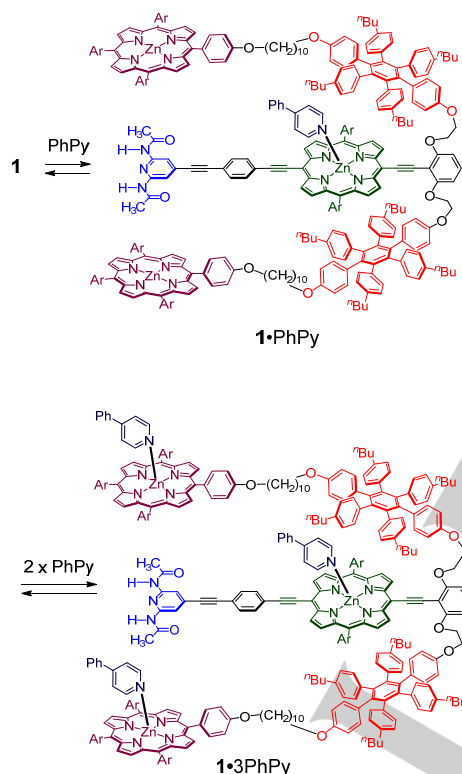


Figure 8. Stepwise formation of **1**•**3PhPy** from **1** via **1**•**PhPy**.

UV-vis spectroscopic titrations using 4-phenylpyridine (PhPy) as a ligand were performed in toluene at 25 °C to evaluate the ligand-binding ability of P2 in **1** in the absence and presence of **2**. An aliquot of the PhPy solution (5.97×10^{-3} M), up to 100 equivalent, was added to the solution of **1** (9.81×10^{-6} M) and the changes in absorption were recorded as shown in Figure 7 (Figure S4). The absorption bands observed at $\lambda_{\text{max}} = 551$, 594, and 655 nm before the addition decreased in intensity and new bands appeared at $\lambda_{\text{max}} = 563$, 605, and 679 nm. Isobestic points were observed at 558, 625, and 664 nm.^[6] These results indicate that PhPy coordinates with both P1 and P2 in **1**. The coordination reaction was analyzed according to the stepwise

reaction model in Figure 8 by global curve-fitting calculations.^[10] The binding constant between P2 in **1** and PhPy ($K_{1\cdot\text{PhPy}}$, eq 1) was determined as $4.75 \pm 0.02 \times 10^4 \text{ M}^{-1}$. Formation constant ($\beta_{1\cdot 3\text{PhPy}}$, eq 2) from **1**•PhPy to **1**•**3PhPy** was estimated as $4.14 \pm 0.05 \times 10^7 \text{ M}^{-2}$.

$$K_{1\cdot\text{PhPy}} = [\mathbf{1}\cdot\text{PhPy}] / ([\mathbf{1}] [\text{PhPy}]) \quad (1)$$

$$\beta_{1\cdot 3\text{PhPy}} = [\mathbf{1}\cdot 3\text{PhPy}] / ([\mathbf{1}\cdot\text{PhPy}] [\text{PhPy}]^2) \quad (2)$$

UV-vis titrations were also performed to determine the binding constants of P2 in **1**•**2** with PhPy (Figure S5). The solution of **1**•**2** was prepared by adding the solution of **2** (6.08×10^{-4} M) to the solution of **1** (9.81×10^{-6} M). The solution of PhPy (5.97×10^{-3} M) was added to the solution of **1**•**2**, up to 100 equivalent, and the spectral change was monitored (Figure 9). The band of P2 at $\lambda_{\text{max}} = 643$ nm (0 equiv) disappeared and a new band at $\lambda_{\text{max}} = 679$ nm (100 equiv) appeared in the titration, indicating the axial coordination of PhPy to P2 in **1**. On the contrary, an insignificant change was observed for the bands at $\lambda_{\text{max}} = 551$ nm where P1 with Py has a dominant absorption. An isobestic point was clearly observed at 658 nm. Overall, these results suggested that the binding between **1** and **2** was maintained in the titration and also the coordination of PhPy to P1 was inhibited in a competitive manner. The 1:1 binding model in Figure 10 was successfully applied to reproduce the observed spectral change by global curve-fitting calculations. The binding constant $K_{1\cdot 2\cdot\text{PhPy}}$ (eq 3) was evaluated as $4.23 \pm 0.02 \times 10^3 \text{ M}^{-1}$.

$$K_{1\cdot 2\cdot\text{PhPy}} = [\mathbf{1}\cdot 2\cdot\text{PhPy}] / ([\mathbf{1}\cdot 2] [\text{PhPy}]) \quad (3)$$

The ratio of the binding constant between ligand and receptor ($K_{1\cdot 2\cdot\text{PhPy}}/K_{1\cdot\text{PhPy}}$) was employed to evaluate the degree of inhibition for the binding between PhPy and P2 in **1**•**2** compared to that of **1**. The smaller values of $K_{1\cdot 2\cdot\text{PhPy}}/K_{1\cdot\text{PhPy}}$ indicate stronger inhibition. The $K_{1\cdot 2\cdot\text{PhPy}}/K_{1\cdot\text{PhPy}}$ was calculated as 0.089 that is significantly smaller than that of the previously reported receptor (0.24).^[6] In spite of the conformational flexibility of the side chains, the sterically bulky shielding panels significantly enhanced the degree of allosteric inhibition. These results established that hexaarylbenzene groups are superior shielding units for covering both faces of P2 to inhibit the axial-ligand coordination on P2.

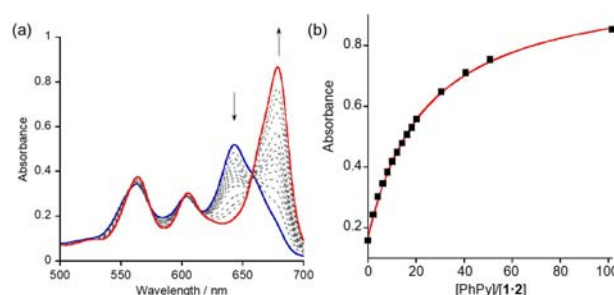


Figure 9. (a) UV-vis spectral change resulting from the titration of **1**•**2** (9.65×10^{-6} M) with 4-phenylpyridine in toluene at 25 °C (blue line: 0 equiv, red line: 100 equiv). (b) The change in the absorbance at 679 nm as a function of concentration of 4-phenylpyridine (black square). The red solid line is a theoretical binding curve obtained by the curve fitting.

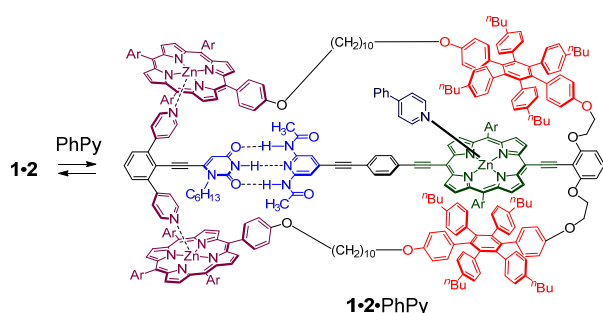


Figure 10. Formation of **1:2•PhPy** from **1:2** and PhPy.

Conclusion

The stimulus-responsive receptor **1** comprising two types of zinc porphyrins P1 and P2 as active sites was prepared. Simultaneous formation of multiple hydrogen and coordination bonds between the receptor **1** and the organic effector **2**, produced the stable supramolecular complex. The ligand-binding ability of P1 was competitively inhibited owing to the high stability of the complex. The multiple supramolecular bonds provided enough driving force for the conformational transformation that plays a key role in allosteric inhibition of P2 activity. The incorporation of sterically bulky shielding units results in considerable enhancement in the degree of allosteric inhibition. The stimulus-responsive shielding for allosteric inhibition presented in this paper is extensively applicable for the development of receptors that can respond to neutral organic effectors. It is notable that only an organic molecule with a specific structure can play as an effector in this system. This feature is also characteristic advantage of the molecular recognition by multiple bonding interactions.

Experimental Section

General Information

Melting points were taken on Yanako MP J-3 apparatus and are uncorrected. NMR spectra were recorded on JEOL JNM-ECZ 400, Bruker AV 300N, and Bruker AV III HD 400 spectrometers. IR spectra were obtained on a JASCO FTIR-4600 spectrometer. The ESI mass was measured on a JEOL AccuTOF LC-plus 4G spectrometer. MALDI-TOF mass was measured on Shimadzu-Kratos AXIMA-CFR Plus and BURUKER solariX spectrometers using dithranol as a matrix reagent. Elemental analyses were obtained from the Analytical Center in Osaka City University. UV-vis spectra were obtained on Shimadzu UV-2550PC spectrometer. TLC was carried out using 0.25 mm thick Wako silica gel (70 F254). Kanto kagaku silica gel 60 (spherical) were used as the stationary phase for column chromatography. Zinc porphyrin **7** was prepared according to the reported methods.^[9] Commercially available reagents and solvents were purified and dried when necessary.

1,4-Diiodo-2,3,5,6-tetrakis(4-butylphenyl)benzene (**4**)

Mg turnings (7.81 g, 321 mmol) were placed in a three-necked flask under a nitrogen atmosphere. After anhydrous THF (150 mL) was added to the flask, 1-bromo-4-butylbenzene (19.0 mL, 111 mmol) was added dropwise in an ice bath. The mixture was stirred at room temperature for

2 h. The solution was decanted into another flask for leaving excess Mg, and hexabromobenzene (**3**) (5.02 g, 9.11 mmol) in 50 mL anhydrous THF was added to the flask. The mixture was stirred at room temperature for 22 h. The mixture was quenched with a 1 M solution of iodine in THF (58.0 mL, 58.0 mmol) and stirred for 15 min. Excess iodine was consumed by the addition of 1 M aqueous Na₂SO₃ and the mixture was extracted from CH₂Cl₂ (400 mL). The organic layer was washed with water (200 mL × 2) and dried over anhydrous Na₂SO₄. The solvent was evaporated under reduced pressure to yield **4** as a white solid (3.86 g, 49%). **4**: m.p. > 300 °C; ¹H NMR (300 MHz, CDCl₃): δ (ppm) 6.94 (d, *J* = 8.3 Hz, 8H; Ar-H), 6.90 (d, *J* = 8.3 Hz, 8H; Ar-H), 2.50 (t, *J* = 7.6 Hz, 8H; ArCH₂), 1.51–1.44 (m, 8H; CH₂), 1.22–1.16 (sext, *J* = 7.4 Hz, 8H; CH₂), 0.871 (t, *J* = 7.4 Hz, 12H; CH₃); ¹³C NMR (100 MHz, CDCl₃): δ (ppm) 146.6, 143.1, 141.3, 129.8, 127.4, 108.4, 35.3, 33.5, 22.2, 14.1; IR (KBr/cm⁻¹) 3047, 3025, 2957, 2926, 2871, 2856, 2357, 2341, 2322, 1516, 1457, 1406, 1376, 1212, 1115, 1026, 833, 644, 553; HRMS (ESI+): calcd for C₄₆H₅₃I₂ *m/z* 859.2237; found *m/z* 859.2232.

4,4''-Butyl-4',5'-bis(4-butylphenyl)-3',6'-bis(4-methoxyphenyl)-1,1':2',1''-terphenyl (**5**)

A mixture of **4** (2.02 g, 2.35 mmol), 4-methoxyphenylboronic acid (1.39 g, 9.21 mmol), Pd(PPh₃)₄ (134 mg, 0.116 mmol), K₂CO₃ (6.42 g, 46.5 mmol), and trioctylmethylammonium chloride (aliquot 336, 28.0 mg, 0.0693 mmol) in degassed toluene (70 mL) were stirred at 100 °C for 7 h under a nitrogen atmosphere. After cooling to room temperature, the mixture was extracted with CH₂Cl₂ (200 mL). The organic layer was washed with water (100 mL × 3) and dried over anhydrous Na₂SO₄. The solvent was evaporated under reduced pressure. The residue was separated by silica gel column chromatography (hexane–CH₂Cl₂ 4:1 (v/v)) to yield **5** as a yellow solid (1.90 g, 98%). **5**: m.p. 94 °C; ¹H NMR (300 MHz, CDCl₃): δ (ppm) 6.70–6.61 (m, 20H; Ar-H), 6.38 (d, *J* = 8.7 Hz, 4H; Ar-H in C₆H₄OMe), 3.60 (s, 6H; OCH₃), 2.36 (t, *J* = 7.3 Hz, 8H; ArCH₂), 1.40 (quin, *J* = 7.3 Hz, 8H; CH₂), 1.14 (sext, *J* = 7.3 Hz, 8H; CH₂), 0.827 (t, *J* = 7.3 Hz, 12H; CH₃); ¹³C NMR (100 MHz, CDCl₃): δ (ppm) 156.9, 140.7, 139.1, 138.4, 133.6, 132.6, 131.4, 126.7, 112.0, 55.0, 35.1, 33.5, 21.9, 14.1; IR (KBr/cm⁻¹) 3047, 3021, 2997, 2955, 2928, 2857, 1610, 1516, 1458, 1287, 1245, 1173, 1038, 1027, 831, 799, 569, 553; HRMS (ESI+): calc for C₆₀H₆₇O₂ *m/z* 819.5141; found *m/z* 819.5168.

2',3',5',6'-Tetrakis(4-butylphenyl)-[1,1':4',1''-terphenyl]-4,4''-diol (**6**)

The solution of BBr₃ in CH₂Cl₂ (1.0 M, 4.1 mL, 4.1 mmol) was added dropwise to **5** (590 mg, 0.720 mmol) in anhydrous CH₂Cl₂ (135 mL) at –20 °C under a nitrogen atmosphere. After stirring at room temperature for 7 h, the mixture was washed with water (100 mL × 3) and dried over anhydrous Na₂SO₄. The solvent was evaporated under reduced pressure to yield **6** as a yellow solid (565 mg, 99%). **6**: m.p. 250–252 °C; ¹H NMR (300 MHz, CDCl₃): δ (ppm) 6.66–6.63 (m, 20H; Ar-H), 6.31 (d, *J* = 8.7 Hz, 4H; Ar-H in C₆H₄OH), 4.26 (s, 2H; OH), 2.36 (t, *J* = 7.4 Hz, 8H; ArCH₂), 1.40 (quin, *J* = 7.4 Hz, 8H; CH₂), 1.15 (sext, *J* = 7.4 Hz, 8H; CH₂), 0.83 (t, *J* = 7.4 Hz, 12H; CH₃); ¹³C NMR (100 MHz, CDCl₃): δ (ppm) 152.7, 140.6, 139.2, 138.3, 133.8, 132.8, 131.4, 126.7, 113.6, 35.1, 33.4, 22.0, 14.1; IR (KBr/cm⁻¹) 3537, 3399, 3024, 2955, 2928, 2871, 2857, 2361, 1900, 1611, 1592, 1517, 1458, 1439, 1420, 1396, 1378, 1263, 1171, 1115, 1101, 1019, 856, 833, 754, 546; HRMS (ESI+): calc for C₅₈H₆₃O₂ *m/z* 791.4828; found *m/z* 791.4857.

Zinc tetraphenylporphyrin **8**

A mixture of porphyrin **7**^[9] (200 mg, 0.194 mmol), 1,10-dibromodecane (0.44 mL, 1.95 mmol), and K₂CO₃ (42.0 mg, 0.304 mmol) in anhydrous DMF (20 mL) were stirred at room temperature for 13 h under a nitrogen atmosphere. The mixture was extracted with CH₂Cl₂ (40 mL). The organic solution was washed with saturated solution of NH₄Cl (20 mL × 2) and water (20 mL × 2) and dried over anhydrous Na₂SO₄. The solvent was evaporated under reduced pressure. The residue was washed with MeOH (40 mL) to yield **8** as a purple solid (212 mg, 87%). **8**: m.p.

291 °C; ¹H NMR (400 MHz, CDCl₃): δ (ppm) 8.99 (d, *J* = 4.2 Hz, 8H; β-H), 8.13 (d, *J* = 8.6 Hz, 2H; Ar-H in C₆H₄OR), 8.09 (d, *J* = 1.8 Hz, 4H; Ar-H in 3,5-BuC₆H₃), 8.08 (d, *J* = 1.8 Hz, 2H; Ar-H in 3,5-BuC₆H₃), 7.78 (m, 3H; Ar-H in 3,5-BuC₆H₃), 7.27 (d, *J* = 8.6 Hz, 2H; Ar-H in C₆H₄OR) 4.26 (t, *J* = 5.1 Hz, 2H; OCH₂), 3.44 (t, *J* = 5.3 Hz, 2H; CH₂Br), 1.99 (quin, *J* = 5.1 Hz, 2H; CH₂), 1.90 (quin, *J* = 5.3 Hz, 2H; CH₂), 1.69–1.59 (m, 2H; CH₂), 1.52 (s, 54H; tBu), 1.42–1.24 (m, 10H; CH₂); ¹³C NMR (100 MHz, CDCl₃): δ (ppm) 158.8, 150.6, 150.5, 148.6, 142.0, 135.4, 135.3, 132.3, 132.0, 129.8, 129.7, 122.5, 120.9, 112.7, 68.4, 35.2, 34.3, 33.0, 31.9, 31.6, 29.7, 29.6, 29.6, 28.9, 28.3, 26.4; IR (KBr/cm⁻¹) 3444, 2962, 2859, 2360, 2341, 1592, 1509, 1474, 1362, 1339, 1290, 1247, 1222, 1173, 1001, 823, 799, 718; HRMS (MALDI-TOF): calcd for C₇₈H₉₅N₄OZn *m/z* 1246.5975; found *m/z* 1246.5969.

Side arm 9

A mixture of **6** (750 mg, 0.948 mmol), **8** (300 mg, 0.240 mmol), K₂CO₃ (165 mg, 1.20 mmol), and 18-crown-6 (16 mg, 0.0667 mmol) in anhydrous DMF (30 mL) were stirred at 50 °C for 23 h under a nitrogen atmosphere. The organic solution was washed with saturated solution of NH₄Cl (60 mL × 2) and water (60 mL × 2) and dried over anhydrous Na₂SO₄. The solvent was evaporated under reduced pressure. The residue was purified by silica gel column chromatography (hexane–CH₂Cl₂ 1:1 (v/v)) to yield **9** as a purple solid (294 mg, 63%). **9**: m.p. 180 °C; ¹H NMR (400 MHz, CDCl₃): δ (ppm) 8.99 (d, *J* = 4.5 Hz, 8H; β-H), 8.12 (d, *J* = 8.6 Hz, 2H; Ar-H in Porphyrin-C₆H₄OR), 8.09 (d, *J* = 1.8 Hz, 4H; Ar-H in 3,5-BuC₆H₃), 8.08 (d, *J* = 1.8 Hz, 2H; Ar-H in 3,5-BuC₆H₃), 7.79–7.78 (m, 3H; Ar-H in 3,5-BuC₆H₃), 7.27 (d, *J* = 8.6 Hz, 2H; Ar-H in Porphyrin-C₆H₄OR), 6.68–6.62 (m, 20H; Ar-H in tBuC₆H₄ and OC₆H₄), 6.39 (d, *J* = 8.8 Hz, 2H; Ar-H in OC₆H₄), 6.30 (d, *J* = 8.6 Hz, 2H; Ar-H in C₆H₄OH), 4.29 (s, 1H; OH), 4.25 (t, *J* = 5.1 Hz, 2H; OCH₂), 3.75 (t, *J* = 5.0 Hz, 2H; OCH₂), 2.38–2.34 (m, 8H; ArCH₂), 1.98 (quin, *J* = 5.1 Hz, 2H; CH₂), 1.70–1.66 (m, 2H; CH₂), 1.64–1.60 (m, 2H; CH₂), 1.52 (s, 54H; tBu), 1.43–1.35 (m, 18H; CH₂), 1.19 (m, 8H; CH₂), 0.85–0.81 (m, 12H; CH₃); ¹³C NMR (100 MHz, CDCl₃): δ (ppm) 158.7, 156.3, 152.6, 150.4, 150.3, 148.5, 141.9, 140.5, 140.5, 139.7, 139.5, 139.0, 138.3, 135.3, 135.1, 133.7, 133.3, 132.7, 132.5, 132.1, 131.8, 131.3, 129.7, 129.6, 126.6, 122.3, 120.7, 113.5, 112.6, 112.5, 71.0, 68.3, 67.7, 66.4, 61.4, 35.0, 33.4, 33.3, 31.7, 29.7, 29.6, 29.6, 29.5, 29.3, 26.2, 26.0, 21.8, 21.8, 15.0, 14.0; IR (KBr/cm⁻¹) 3444, 2955, 2928, 2858, 2360, 1608, 1592, 1515, 1466, 1393, 1362, 1339, 1286, 1244, 1173, 1001, 824, 798, 718, 547; HRMS (MALDI-TOF): calc for C₁₃₆H₁₅₆N₄O₃Zn *m/z* 1957.1463; found *m/z* 1957.1448.

Receptor 1

Under a nitrogen atmosphere a mixture of side arm **9** (110 mg, 0.0561 mmol), main unit **10**^[6] (34mg, 0.0226 mmol), K₂CO₃ (19 mg, 0.138 mmol), and 18-crown-6 (4.1 mg, 0.0152 mmol) in anhydrous acetone (4 mL) were stirred at under reflux for 23 h. The organic solution was washed with saturated solution of NH₄Cl (60 mL × 2) and water (60 mL × 2) and dried over anhydrous Na₂SO₄. The solvent was evaporated under reduced pressure. The residue was separated by silica gel column chromatography (hexane–CH₂Cl₂ 1:1 (v/v)) to yield **1** as a purple solid (33 mg, 28%). **1**: m.p. > 300 °C; ¹H NMR (600 MHz, CDCl₃): δ (ppm) 9.87 (d, *J* = 4.3 Hz, 2H; β-H in P2), 9.77 (d, *J* = 4.3 Hz, 2H; β-H in P2), 9.04–8.98 (m, 18H; β-H in P1 and P2), 8.92 (d, *J* = 4.3 Hz, 2H; β-H in P2), 8.14–8.06 (m, 22H; Ar-H in P1 and P2, NH), 8.02 (d, *J* = 7.8 Hz, 2H; Ar-H) 7.85 (br, 2H; Py-H), 7.82–7.77 (m, 8H; Ar-H in P1 and P2, Ar-H), 7.74 (d, *J* = 7.8 Hz, 2H; Ar-H), 7.30 (m, 1H; Ar-H), 7.27 (overlap with solvent peak, 4H; Ar-H in P1), 6.75 (d, *J* = 8.5 Hz, 2H; Ar-H), 6.74–6.49 (m, 40H; Ar-H in the shielding units), 6.40 (d, *J* = 8.9 Hz, 4H Ar-H in the shielding units), 6.31 (d, *J* = 7.9 Hz, 4H Ar-H in the shielding units), 4.58 (m, 4H; OCH₂CH₂O), 4.53 (m, 4H; OCH₂CH₂O), 4.24 (t, *J* = 6.3 Hz, 4H; OCH₂), 3.75 (t, *J* = 6.4 Hz, 4H; OCH₂), 2.40–2.30 (m, 12H; ArCH₂, CH₂), 2.04–1.94 (m, 18H; ArCH₂, CH₂, OCH₃), 1.73–1.42 (m, 152H; tBu, 2×CH₂), 1.42–1.20 (m, 12H; CH₂ in tBu, 2×CH₂), 1.40–1.17 (m, 16H; 2×CH₂ in tBu), 1.17–0.99 (m, 8H; CH₂ in tBu), 0.89–0.76 (m, 20H; CH₂, CH₃ in

tBu), 0.63–0.57 (m, 12H; CH₃ in tBu), (see Figures S9 and S10 for peak assignment); ¹³C NMR (100 MHz, CDCl₃): δ (ppm) 160.9, 158.8, 156.3, 155.7, 152.1, 151.9, 150.5, 150.4, 150.4, 149.1, 148.8, 148.5, 141.9, 141.3, 140.4, 139.7, 139.5, 138.9, 138.8, 138.3, 138.2, 135.3, 135.2, 134.2, 133.4, 133.1, 132.6, 132.5, 132.3, 132.1, 131.8, 131.5, 131.3, 131.2, 130.0, 129.7, 129.59, 126.57, 126.5, 124.3, 122.3, 121.0, 120.7, 113.0, 112.7, 112.6, 111.2, 68.3, 67.8, 66.3, 35.1, 35.0, 34.8, 33.3, 33.1, 31.9, 31.8, 29.7, 29.59, 29.57, 29.5, 29.4, 29.3, 26.3, 26.1, 24.6, 22.7, 21.8, 21.6, 14.1, 13.9, 13.8; IR (KBr/cm⁻¹) 3428, 2957, 2928, 2859, 2360, 2342, 1735, 1716, 1608, 1593, 1557, 1513, 1465, 1418, 1362, 1286, 1242, 1173, 1112, 1068, 1001, 930, 825, 798, 717; MS (MALDI-TOF) *m/z* 5169.0 [M⁺]; Anal. Calcd. for C₃₅₁H₃₈₅N₁₅O₁₀Zn₃·H₂O: C, 80.98; H, 7.53; N, 4.04; found: C, 80.74; H, 7.60; N, 3.77.

UV-vis spectroscopic titration

UV-vis absorption spectra were measured at 25 °C using 1 cm quartz cuvettes. A solution of a receptor in toluene (3.0 mL, conc. in Table S1) was prepared by careful weighting using an analytical balance. The solution of **1·2** was prepared by adding the solution of **2** to the solution of **1** (Table S1, entry 3). Stock solutions of an external axial ligand in toluene (conc. in Table S1) were also prepared. The binding constant was determined according to the following procedure. The stock solution of the ligand was repeatedly added to the solution of the receptor in the cuvette by using a micro pipette (*V*_{add} in Table S1) and the solution was stirred. After each addition the cuvette was placed in the cell compartment of a spectrometer and allowed to come to temperature equilibrium. UV-vis absorption spectra were measured with a Shimadzu UV-2550PC spectrometer equipped with a temperature controller. This procedure was repeated until no change was recorded within the spectra. UV-vis spectrophotometric titrations were globally analysed by curve-fitting the 500–700 nm region of spectra at 1 nm intervals using the software ReactLab EQUILIBRIA.^[12]

Acknowledgements

This work was partially supported by Grant-in-Aid for Scientific Research (JSPS KAKENHI #Grant Numbers, JP15H00956 (K.O.) JP17K05790 (M.K. and K.O.) and JP26102005 (S.S), JP17K05783 (S.S)).

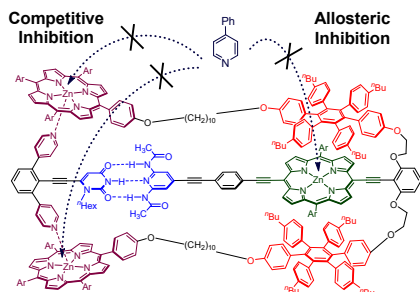
Keywords: Porphyrinoids • Allosterism • Supramolecular chemistry • Receptors • Molecular recognition

- [1] M. F. Perutz, *Molecular Mechanisms of Cooperativity and Allosteric Regulation in Proteins*, Cambridge University Press, **1990**.
- [2] (a) C. Kremer, A. Lützen, *Chem.–Eur. J.* **2013**, *19*, 6162–6196; (b) A. M. Lifschitz, M. S. Rosen, C. M. McGuirk, C. A. Mirkin, *J. Am. Chem. Soc.* **2015**, *137*, 7252–7261; (c) T. Nabeshima, *Bull. Chem. Soc. Jpn.* **2010**, *83*, 969–991; (d) A. J. McConnell, C. S. Wood, P. P. Neelakandan, J. R. Nitschke, *Chem. Rev.* **2015**, *115*, 7729–7793; (e) N. Mittal, S. Pramanik, I. Paul, S. De, M. Schmitt, *J. Am. Chem. Soc.* **2017**, *139*, 4270–4273; (f) N. Mittal, M. S. Özer, M. Schmitt, *Inorg. Chem.* **2018**, *57*, 3579–3586; (g) I. Paul, A. Goswami, N. Mittal, M. Schmitt, *Angew. Chem., Int. Ed.* **2018**, *57*, 354–358; *Angew. Chem.* **2018**, *130*, 360–364.
- [3] (a) M. J. Wiest, P. A. Ulmann, C. A. Mirkin, *Angew. Chem., Int. Ed.* **2011**, *50*, 114–137; *Angew. Chem.* **2011**, *123*, 1453–1481; (b) M. Kozaki, Y. Ninomiya, S. Suzuki, K. Okada, *Tetrahedron Lett.* **2013**, *54*, 3658–3661; (c) M. Schmitt, S. De, S. Pramanik, *Angew. Chem., Int. Ed.* **2012**, *51*, 3832–3836; *Angew. Chem.* **2012**, *124*, 3898–3902; (d) V. Marcos, A. J. Stephens, J. Jaramillo Garcia, A. L. Nussbaumer, S. L. Woltering, A. Valero, J. F. Lemonnier, I. J. Vitorica Yrezabal, D. A. Leigh, *Science* **2016**, *352*, 1555–1559; (e) M. Kato, E. Hashimoto, M. Kozaki, S. Suzuki, K. Okada, *Tetrahedron Lett.* **2012**, *53*, 309–312.

- [4] (a) H. Kawai, R. Katoono, K. Nishimura, S. Matsuda, K. Fujiwara, T. Tsuji, T. Suzuki, *J. Am. Chem. Soc.* **2004**, *126*, 5034–5035; (b) H. Sato, K. Tashiro, H. Shinmori, A. Osuka, Y. Murata, K. Komatsu, T. Aida, *J. Am. Chem. Soc.* **2005**, *127*, 13086–13087; (c) J. Heo, C. A. Mirkin, *Angew. Chem., Int. Ed.* **2006**, *45*, 941–944; *Angew. Chem.* **2006**, *118*, 955–958; (d) J. Rio, S. Beeck, G. Rotas, S. Ahles, D. Jacquemin, N. Tagmatarchis, C. Ewels, H. A. Wegner, *Angew. Chem., Int. Ed.* **2018**, *57*, 6930–6934; *Angew. Chem.* **2018**, *130*, 7046–7050; (e) S.-Y. Chang, H.-Y. Jang, K.-S. Jeong, *Chem. Eur. J.* **2004**, *10*, 4358–4366; (f) J. S. Park, F. Le Derf, C. M. Bejger, V. M. Lynch, J. L. Sessler, K. A. Nielsen, C. Johnsen, J. O. Jeppesen, *Chem.–Eur. J.* **2010**, *16*, 848–854.
- [5] H. J. Yoon, J. Kuwabara, J.-H. Kim, C. A. Mirkin, *Science* **2010**, *330*, 66–69.
- [6] Y. Sasaki, S. Suzuki, K. Okada, M. Kozaki, *Tetrahedron Lett.* **2016**, *57*, 4082–4085.
- [7] Y. Ninomiya, M. Kozaki, S. Suzuki, K. Okada, *Bull. Chem. Soc. Jpn.* **2014**, *87*, 1195–1201.
- [8] (a) S. Shah, B. E. E. Eichler, R. C. Smith, P. P. Power, J. D. Protasiewicz, *New. J. Chem.* **2003**, *27*, 442–445; (b) X. Yang, X. Dou, K. Müllen, *Chem. Asian J.* **2008**, *3*, 759–766.
- [9] (a) H. Yamada, H. Imahori, S. Fukuzumi, *J. Mater. Chem.* **2002**, *12*, 2034–2040; (b) M. Kozaki, A. Uetomo, S. Suzuki, K. Okada, *Org. Lett.* **2008**, *10*, 4477–4480.
- [10] A. Uetomo, M. Kozaki, S. Suzuki, K. Yamanaka, O. Ito, K. Okada, *J. Am. Chem. Soc.* **2011**, *133*, 13276–13279.
- [11] (a) R. Kimura, S. Suzuki, K. Okada, M. Kozaki, *J. Org. Chem.* **2017**, *82*, 8917–8926; (b) M. Akisada, R. Kimura, Y. Tachi, S. Suzuki, K. Okada, M. Kozaki, *J. Org. Chem.* **2018**, *83*, 9631–9640; (c) R. Kimura, S. Suzuki, K. Okada, M. Kozaki, *Chem. Asian J.* **2018**, *13*, 35–40.
- [12] Program ReactLab Equilibria, Jplus consulting Pty Ltd. In the region with the higher [1]/[2] values, the absorption gradually decreased due to the dilution.
- [13] (a) L. Đorđević, T. Marangoni, T. Miletić, J. Rubio-Magnieto, J. Mohanraj, H. Amenitsch, D. Pasini, N. Liaros, S. Couris, N. Armaroli, M. Surin, D. Bonifazi, *J. Am. Chem. Soc.* **2015**, *137*, 8150–8160; (b) K. Hager, U. Hartnagel, A. Hirsch, *Eur. J. Org. Chem.* **2007**, 1942–1956; (c) S. Shinoda, M. Ohashi, H. Tsukube, *Chem.–Eur. J.* **2007**, *13*, 81–89.

Entry for the Table of Contents

Insert graphic for Table of Contents here. ((Please ensure your graphic is in **one** of following formats))



A stimulus-responsive receptor was prepared to control the ligand-binding ability of three active sites with one effector. A stable supramolecular complex of the receptor and the effector was produced via the cooperative formation of multiple hydrogen and coordination bonds. As the result, the binding of a ligand to the active sites was inhibited in a competitive and allosteric mechanism.

Institute and/or researcher Twitter usernames: ((optional))